

SYNAPTOLOGY OF THE NIGROSTRIATAL PROJECTION IN RELATION TO THE COMPARTMENTAL ORGANIZATION OF THE NEOSTRIATUM IN THE RAT

J. J. HANLEY* and J. P. BOLAM

MRC Anatomical Neuropharmacology Unit, Department of Pharmacology, Mansfield Road,
Oxford, U.K.

Abstract—The patch-matrix organization of the striatal complex, which is fundamental to the structural and functional organization of the basal ganglia, is characterized on the basis of both connections and neurochemistry. In order to determine whether differences in the connections and neurochemistry are reflected in differences in synaptic organization, we examined the synaptology of the dopaminergic nigrostriatal projection in the patch-matrix complex of the rat. Three approaches were used. First, deposits of the anterograde tracer, biotinylated dextran amine, were placed in the substantia nigra. Sections of perfuse-fixed neostriatum were then processed to reveal anterogradely-labelled nigrostriatal axons and calbindin-D28k immunoreactivity, a marker for the patch-matrix complex. Secondly, sections of perfuse-fixed neostriatum were immunolabelled to reveal both tyrosine hydroxylase, a marker for dopaminergic structures and calbindin-D28k. Labelled axons in the patches and the matrix were examined at both the light and the electron microscopic levels. Finally, in order to test for the presence of fixed GABA in sub-types of anterogradely-labelled terminals in the neostriatum, ultrathin sections were immunolabelled by the post-embedding immunogold method.

Based on morphological analysis, anterogradely-labelled nigrostriatal axons were divided into two types (Type I and Type II). The density of tyrosine hydroxylase labelling in the neostriatum prevented the classification of immunolabelled nigrostriatal axons. The Type I anterogradely-labelled axons and tyrosine hydroxylase-positive axons were found both in the patches and in the matrix. They both formed symmetrical synapses with spines, dendrites and occasionally somata. The morphology, dimensions, type of synaptic specialization and the distribution of postsynaptic targets of axons labelled by both methods were similar in the patches and the matrix. The Type I anterogradely-labelled axons were immunonegative for GABA. The Type II anterogradely-labelled axons were GABA-immunopositive, were found only in the matrix and were only present in those animals in which retrograde labelling was observed in the globus pallidus, they are thus not part of the dopaminergic nigrostriatal projection.

It is concluded that although the patch-directed and matrix-directed dopaminergic projections from the ventral mesencephalon arise from different populations of dopaminergic neurons, their innervation of neurons in the patches and matrix is similar. The anatomical substrate, and therefore probably also the mechanism, for dopaminergic modulation of the flow of cortical information through the striatal complex is essentially the same in the patch and in the matrix sub-divisions of the striatal complex. © 1997 IBRO. Published by Elsevier Science Ltd.

Key words: striosome, patch, matrix, anterograde tracing, immunocytochemistry.

The basal ganglia, which are a group of extensively interconnected subcortical nuclei, are involved in a variety of higher functions including motor control, memory and cognition.^{2,13,14,17,33,35,43,82} The neostriatum, which is a major division of the basal ganglia, is homogeneous at the cellular level, consisting of between 90% and 95% of a single morphological type of neuron, i.e. the medium spiny projection neuron.^{53,70} However, the neostriatum exhibits

several levels of heterogeneity, the most prominent of which, apart from the gross topography of projections to the neostriatum, is the striosome or patch-matrix complex. This organizational principle was originally defined on the basis of neurochemical heterogeneities³⁹ and subsequently shown to be related to differences in neostriatal connectivity.^{4,21,26,38,44,46,66} The patches and the matrix occupy 15% and 85% of the neostriatal volume, respectively,⁴⁷ and are complementary, interdigitating compartments, the patches forming a labyrinthine three-dimensional structure embedded within the matrix.^{34,41}

Many transmitter-related markers and other neurochemicals respect the patch-matrix compartmentalization, such that they are either enriched in the

*To whom correspondence should be addressed.

Abbreviations: ABC, avidin-biotin-peroxidase complex; BDA, biotinylated dextran amine; DAB, diaminobenzidine; PAP, peroxidase-antiperoxidase; PB, phosphate buffer; PBS, phosphate-buffered saline; TB, Tris buffer; TBS, Tris-buffered saline; TBS-Triton, Tris-buffered saline with 0.01% Triton X-100.

patches and weak in the matrix or vice versa. For example, patches are relatively weak in acetylcholinesterase activity,³⁹ calbindin-D28k immunoreactivity,³⁰ choline acetyltransferase-immunoreactive fibres,³⁷ somatostatin-immunoreactive fibres,^{15,26} parvalbumin-immunoreactive fibres (in primates),^{6,60,79} and are relatively enriched in μ -opioid receptors,⁴⁴ M1 muscarinic receptors⁵⁹ and calretinin-immunoreactive fibres (in primates).⁶⁰

Overlying the neurochemical differences, and indeed partly responsible for them, are structural differences that relate to the location of neostriatal neurons and their axodendritic architecture. Thus, dendrites and local axon collaterals of spiny projection neurons generally remain within the compartment in which the cell body resides.^{10,51,52,63,80,81} In contrast, although the somata of somatostatin-immunoreactive striatal interneurons and cholinergic interneurons are found both within the patches and the matrix, their axonal arborization is mainly within the matrix.^{15,26,37,49,50,55,68} Furthermore, the morphology of GABA interneurons in the primate, defined on the basis of parvalbumin immunoreactivity, show marked differences between the patches and the matrix.⁶

The organization of many of the afferent and efferent connections of the neostriatum are also related to the patch-matrix complex.^{22,27,28,31,46,56,67} Thus, neurons of the matrix project to the globus pallidus and/or basal ganglia output nuclei, whereas neurons of the patches selectively terminate in the ventral tier of the substantia nigra pars compacta and the rostral entopeduncular nucleus. Many of the main afferents of the neostriatum show selectivity in the innervation of the patches or the matrix. For example, neurons in deep layer V and layer VI of the cortex selectively innervate patches, whereas neurons located in upper layer V and layer III selectively innervate the matrix.^{7,28} Similarly, dopamine neurons located in the dorsal tier of the substantia nigra pars compacta preferentially project to the matrix, whereas dopamine neurons of the ventral tier preferentially project to the patches.^{31,46}

These clear neurochemical, structural and connective differences between the patches and the matrix raise the possibility that differences may also exist in the synaptology of neostriatal neurons, implying that there are differences in the way that information is processed in the two compartments. In view of the differential origin of the dopaminergic input to the patch and matrix and its importance in both the physiology^{18,33,36} and pathophysiology^{1,16} of the basal ganglia, the object of the present study was to determine whether differences exist in the synaptology of the dopaminergic nigrostriatal input to neurons of the patch and matrix compartments. This was addressed at the light and electron microscopic levels by labelling nigrostriatal terminals either immunocytochemically or by anterograde labelling, in combination with immunocytochemistry for

calbindin-D28k, a marker for the patch-matrix complex.

EXPERIMENTAL PROCEDURES

Twenty male Sprague-Dawley rats (250–350 g; Charles River, U.K.) were used in the present study. They were maintained on a 12 h light/12 h dark cycle with free access to food and water. Environmental conditions for housing of the rats, and all procedures that were performed on them, were in accordance with the Animals (Scientific Procedures) Act 1986. All surgical procedures were carried out under aseptic conditions and deep anaesthesia, which was induced and maintained by intra-peritoneal injections of a neuroleptanalgesic consisting of fentanyl/fluanison (Hypnorm; Janssen) and midazolam (Hypnovel; Roche) (1:1:2 with sterile water; 2.7 ml/kg).

Iontophoretic injection of neuronal tracer

Bilateral deposits of anterograde tracer were placed in the substantia nigra ($n=15$) using stereotaxic co-ordinates derived from the atlas of Paxinos and Watson.⁶² Rostro-caudal and mediolateral co-ordinates were calculated using Bregma as the stereotaxic reference point. Access to the brain was made using a dental drill to create a burr hole in the cranium. Dorsoventral co-ordinates were calculated from the dural surface prior to cutting of the dura to facilitate the entry of the glass micropipette into the brain. Biotinylated dextran amine (BDA; 10% in 0.9% NaCl; Molecular Probes, U.S.A.)⁷⁷ was delivered by iontophoresis into the substantia nigra via glass micropipettes of 7–50 μ m internal tip diameter using a pulsed (7 s on/7 s off) cathodal current (0.5–10 μ A) over 10–20 min. Following the injection of the anterograde tracer, the glass micropipettes were left *in situ* for at least 10 min to minimize leakage along the injection track. The skin overlying the exposed cranium was then drawn together and sutured. The animals were kept warm and allowed to fully recover from the anaesthetic in isolation before being returned to the home cage.

Perfusion fixation

Animals that received injections of anterograde tracer were allowed to survive for five to eight days. They were then deeply anaesthetized with sodium pentobarbitone (Sagatal; 60 mg/kg, i.p.). Blood was removed from the brain by rapid transcardial perfusion with phosphate-buffered saline (PBS; 0.01 M, pH 7.4; 50–100 ml) over 1–2 min using a peristaltic pump. They were then perfused with 300 ml of 0.2–0.5% glutaraldehyde ($n=13$) and 2–4% paraformaldehyde in phosphate buffer (PB; 0.1 M, pH 7.4) over 30 min. Two animals were perfused for 30 min with 300 ml of 1.0% glutaraldehyde and 2% paraformaldehyde in PB. These animals were used to test for the presence of fixed GABA by the post-embedding immunogold method. Following fixation, the brain was removed from the cranium, divided into 5-mm-thick coronal slices and stored in PBS at 4°C prior to further processing. Coronal sections (70 μ m) of the injection site and the neostriatum were taken using a vibrating microtome and collected in PBS. All sections were washed in PBS prior to further processing.

Visualization of neuronal tracer within the substantia nigra

Sections that included the substantia nigra were incubated for 30 min in 0.2% Triton X-100 in PBS. The BDA deposit was visualized by incubation of the sections in an avidin-biotin-peroxidase complex (ABC; 1:100 dilution; Vector Laboratories, U.K.) in PBS containing 0.2% Triton X-100 at room temperature for 4–6 h. Peroxidase linked to BDA by the avidin-biotin bridge was revealed by equilibrating the sections in Tris buffer (TB; 0.05 M, pH 7.6) for 5–10 min and then placing them in TB containing 0.025%

diaminobenzidine (DAB; Sigma, Dorset, U.K.) and 0.006% hydrogen peroxide for 10–15 min. The reaction was terminated by rinsing several times in TB. Alternatively, Vector VIP (Vector Laboratories, U.K.) was used to visualize the BDA by placing the sections in PBS containing the chromogen and hydrogen peroxide, at concentrations specified by the supplier, for 5–15 min. The reaction was terminated by rinsing several times in PBS. Sections containing the injection site were further processed to reveal tyrosine hydroxylase-positive neurons as detailed below.

Visualization of tyrosine hydroxylase-positive neurons in the substantia nigra

Sections of the substantia nigra were incubated in rabbit anti-tyrosine hydroxylase (1:1000; Eugene Tech, U.S.A.) overnight at room temperature. After several washes in PBS, the sections were incubated in a solution of goat anti-rabbit IgG (1:200; DAKO, U.K.) for 2 h at room temperature, followed by a 1 h incubation in rabbit peroxidase-antiperoxidase (PAP; 1:100; DAKO, U.K.). Bound peroxidase was revealed using the chromogen Vector SG or Vector VIP for 5–15 min. On completion of the immunostaining, the sections containing the injection sites were processed for either electron microscopy (see below) or for light microscopy. Sections processed for light microscopy containing the injection site were mounted on gelatine-coated microscope slides, air dried overnight at room temperature, rapidly dehydrated through a graded series of dilutions of alcohol, and a coverslip applied using XAM (Merck, U.K.) as the mounting medium.

Visualization of anterograde labelling within the neostriatum

Sections of neostriatum were cryoprotected and freeze-thawed as described previously.⁷⁸ As these sections were being processed for electron microscopy, Triton X-100 was omitted from the protocol. Anterograde labelling in the neostriatum was visualized by incubation of the sections in ABC complex (1:100) overnight at room temperature and revealed using DAB as the chromogen (as described above). These sections were further processed to reveal calbindin immunoreactivity as a marker of the patch-matrix complex.

Visualization of the patch-matrix complex in the neostriatum

To reveal the patch-matrix organization of the neostriatum, the sections were incubated in mouse monoclonal antibodies raised against calbindin D-28k (1:500; SWant, Switzerland) overnight at room temperature. After several washes in PBS, the sections were incubated in a solution of goat anti-mouse IgG (1:200; DAKO, U.K.) for 2 h at room temperature, followed by a 1 h incubation in mouse monoclonal PAP (1:100; DAKO, U.K.). Bound peroxidase was revealed using the chromogen Vector SG for 5–15 min. They were then processed for electron microscopy.

Double immunocytochemistry for tyrosine hydroxylase and calbindin

Sections of the neostriatum from five animals which did not receive tracer injections, but were similarly perfuse-fixed with 0.05%–0.5% glutaraldehyde and 4% paraformaldehyde, were processed to reveal both tyrosine hydroxylase and calbindin immunoreactivity. Immunocytochemistry was conducted in sequence, with tyrosine hydroxylase being visualized first (as above), using DAB as the chromogen. Calbindin was then visualized (as above) using Vector SG as the chromogen.

Controls for single and double immunocytochemistry

In control experiments for single immunocytochemistry, the primary antibody was omitted. This procedure resulted in a lack of immunocytochemical labelling at the light microscopic level. Labelling at the light microscopic level

for each of the antigens was consistent with many previous observations regardless of which chromogen was used.

In protocols requiring the sequential use of different chromogens, it is important to demonstrate that there are no interactions between the chromogens that would affect the ability to distinguish them at the electron microscopic level. In particular, it was important to ensure the DAB and Vector SG reaction products were distinguishable. Control sections that were not exposed to primary antibody against tyrosine hydroxylase or did not contain transported BDA were subjected to the remainder of the labelling protocol to ensure that the exposure to DAB did not affect the Vector SG reaction product. Under both conditions, no obvious DAB reaction product was visible at the light microscopic level. All sections were then processed for calbindin immunolabelling using Vector SG as the chromogen and were subsequently processed for electron microscopy. Electron microscopic analysis in a blind test conducted by two investigators revealed a weak, slightly electron dense reaction product overlying somata, large dendrites and axon terminals in the matrix. This Vector SG reaction product was clearly distinguishable from that of DAB and its distribution conformed to that of calbindin as described previously.²⁰

Processing of sections for correlated light and electron microscopy

The labelled sections of the neostriatum were placed flat at the bottom of a petri dish and post-fixed in 1% osmium tetroxide (Oxkem, U.K.) in 0.1 M PB at pH 7.4 for 30 min. The sections were then washed in PB and dehydrated through a graded series of dilutions of either alcohol or acetone (10 min).⁸⁶ The sections were treated with propylene oxide (2 × 10 min) and immersed in resin (Durcupan; Fluka, U.K.) overnight at room temperature. Finally, the resin-impregnated sections were mounted on microscope slides, a coverslip was applied, and they were placed in an oven to polymerize the resin at 60°C for 48 h.

Analysis of material

All the sections of the neostriatum that contained anterogradely-labelled structures and sections that were double-labelled to reveal both tyrosine hydroxylase and calbindin immunoreactivity were examined at the light microscopic level. Samples of anterogradely-labelled (from four animals) and tyrosine hydroxylase-positive axons (from four animals) in both the patch and matrix were drawn and/or photographed. Regions of sections that were characterized as being patch or matrix by the calbindin immunostaining and contained anterogradely-labelled or tyrosine hydroxylase-positive elements, were cut from the microscope slides and glued to blank cylinders of resin. These were then trimmed to include only patch or only matrix. Serial ultrathin sections were cut on a Reichert-Jung Ultracut-E ultramicrotome and collected on Pioloform-coated copper or gold slot grids (Agar, U.K.). The ultrathin sections were then contrasted with lead citrate for 1–2 min and examined in a Philips CM410 electron microscope.

To determine the nature of the postsynaptic targets in the patches and matrix of both the anterogradely labelled and of the tyrosine hydroxylase-positive terminals, all parts of ultrathin sections were scanned at a constant magnification. In both the patch and the matrix, all labelled terminals forming synaptic contacts were classified according to their type of specialization and the nature of their postsynaptic target.

An index of the size of both anterogradely-labelled Type I and Type II terminals and tyrosine hydroxylase-immunolabelled terminals was taken as the diameter of labelled structures at the level of, and perpendicular to, the synaptic specialization. Statistical analysis of all data, except where stated, was carried out using the non-parametric Mann-Whitney *U*-test and the Kruskal-Wallis

ANOVA and a level of $P < 0.05$ was considered significant. Analysis of the distribution of postsynaptic elements in the patches and matrix was carried out using Chi-squared test. All values were expressed as a mean value \pm S.E.M.

Post-embedding immunocytochemistry for GABA

In order to test for the presence of fixed GABA in anterogradely labelled terminals in the neostriatum of the BDA-injected animals, ultrathin sections were collected in series on gold, Pioloform-coated grids and labelled by the post-embedding immunogold method. Immunoreactivity for GABA was revealed using a slight modification of the method described by Phend and co-workers.⁶⁴ The grids were first washed in TB (0.05 M, pH 7.6) containing 0.9% NaCl (TBS) and 0.01% Triton X-100 (TBS-Triton) and then incubated overnight at room temperature on drops of a 1:5000 dilution of rabbit anti-GABA antiserum (code 9;^{45,73,74}) in TBS-Triton. After several washes in TBS-Triton, and one wash in TBS at pH 8.2, the grids were incubated for 1 h at room temperature in a 1:25 dilution of 15 nm gold-conjugated goat anti-rabbit IgG (BioCell, U.K.) in TBS (pH 8.2). The grids were washed in TBS (pH 8.2), followed by filtered distilled water, were subsequently stained with 1% aqueous uranyl acetate for 1 h, and finally with lead citrate (1–2 min) prior to examination at the electron microscopic level.

Analysis and quantification of GABA-immunolabelled material

Immunoreactivity for GABA was detected by the presence of electron dense immunogold particles overlying individual neuronal structures. In order to quantify the immunoreactivity in Type I and Type II anterogradely-labelled terminals, the cross-sectional areas of boutons and blood vessels in micrographs were calculated with the aid of a digitizing pad and MacStereology software. These values were then used to calculate the density (particles/ μm^2) of immunogold particles overlying anterogradely-labelled and non-labelled boutons or terminals. The densities were corrected for non-specific binding of the antibodies to tissue-free resin by subtracting the immunogold density overlying the lumen of capillaries in the same ultrathin section. The corrected density of immunogold particles overlying terminals and boutons in GABA-labelled sections was normalized by expressing it as a ratio to that associated with boutons forming asymmetrical synapses, which have previously been shown to be glutamatergic. These values are referred to as the index of GABA immunoreactivity. Issues concerning the quantification of immunolabelling have been discussed extensively on a previous occasion.⁸ The GABA immunoreactivity of bouton samples were compared statistically using the non-parametric Mann-Whitney *U*-test and a level of $P < 0.05$ was considered significant.

RESULTS

Light microscopic observations

Injection site. At the level of the substantia nigra structures labelled with BDA and visualized using Vector VIP, were characterized by the presence of a purple/black homogeneous reaction product which filled neurons and their processes in a Golgi-like fashion at the edges of the injection site. When DAB was used as the chromogen BDA-labelled structures were characterized by the presence of the brown, homogeneous DAB reaction product. Neurons at the centre of the injection site were not usually visible due to the presence of a large amount of reaction product

in the neuropil. Tyrosine hydroxylase-positive neurons of the substantia nigra pars compacta, the displaced tyrosine hydroxylase-positive neurons within the pars reticulata and neurons within the ventral tegmental area were revealed using Vector SG as the chromogen which gave a homogeneous blue reaction product that was distinguishable from the DAB reaction product.

The deposits of BDA were localized in the substantia nigra, principally at the rostrocaudal level of the medial terminal nucleus accessory optic tract (approximately 5.2 mm caudal to the Bregma), and varied along the mediolateral axis. The deposits of BDA ranged in size from 5–10 neurons to a large volume of the substantia nigra pars reticulata (Fig. 1). No BDA reaction product was detected in the crus cerebri or the ventral tegmental area. Occasionally, BDA reaction product was observed along the injection track.

Anterograde labelling in the neostriatum.

Anterogradely-transported BDA in the neostriatum was characterized by the presence of the brown DAB reaction product that filled axons and axonal boutons (Figs 2A–C, 4B). These DAB-labelled, BDA-positive structures were easily discernible from the superficial blue reaction product of the Vector SG that was used to visualize calbindin-immunoreactive structures (Fig. 2A',B',D). Anterograde labelling was also detected in the superior colliculus and the thalamus. Anterograde labelling in the neostriatum revealed a medial-to-medial and lateral-to-lateral topography in the nigrostriatal projection that is consistent with previous findings.^{5,23} Large deposits of the BDA (e.g., deposit numbers 3, 11, 15 in Fig. 1) produced labelling throughout the rostrocaudal extent of the neostriatum, however, the smallest deposit of tracer (5–10 neurons) in the rostral substantia nigra (deposit number 1 in Fig. 1), produced anterograde labelling localized to only the rostral extent of the neostriatum.

The morphology of anterogradely-labelled axons in the neostriatum. Axons located within the neostriatum following the deposit of neuronal tracer within the substantia nigra were categorized into two classes based on their morphology at the light microscopic level.

- (1) Type I fibres formed dense, tortuous networks of fine, varicose axons (Fig. 2A,B). The varicosities were only slightly larger than the axon itself and were irregularly spaced. Type I axons were found distributed to varying degrees, along the full rostrocaudal extent of the neostriatum. They were found in both the patch and the matrix compartments, as defined by the calbindin immunolabelling (Fig. 2A,A',B,B').
- (2) Type II fibres were thicker than Type I fibres and gave rise to numerous grape-like varicosities (Fig. 2C). They were occasionally

observed to outline the somata of unstained neurons. (Fig. 4B). Type II fibres were only found in the matrix following the larger deposits of BDA in the substantia nigra. Structures with a morphology similar to Type II fibres were not detected in material immunolabelled for tyrosine hydroxylase (see below).

Retrograde-labelling following deposit of biotinylated dextran amine. In addition to anterograde labelling, the larger injections of BDA in the substantia nigra resulted in retrograde labelling of neurons in the globus pallidus (Fig. 5A) which was usually in the form of a light, homogeneous, or occasionally a granular stain, filling the somata and primary dendrites. In general, retrogradely-labelled neurons were sparse (2–10 neurons) and were not observed following the smaller deposits of tracer (5–10 neurons) in the substantia nigra. Retrograde labelling of neurons in the globus pallidus was also associated with the labelling of what were assumed to be local axon collaterals.

Neurons in the neostriatum were also retrogradely labelled (1–5 neurons) following larger injections of BDA in the substantia nigra (e.g., deposits number 11 and 15 in Fig. 1). This retrograde labelling filled the somata and primary dendrites with a light, homogeneous stain. These retrogradely-labelled neurons were found mainly in the ventral neostriatum.

Double immunostained sections of neostriatum. In the sections double-labelled to reveal both tyrosine hydroxylase- and calbindin-immunoreactivities, the neostriatum was densely stained by peroxidase reaction products that displayed different colours. Tyrosine hydroxylase labelling dispersed evenly across the entire neostriatum and hence the patch-matrix complex (Fig. 2D). The morphology and trajectory of individual tyrosine hydroxylase-positive axons could not be easily analysed because of the high density of immunolabelled structures. The calbindin-positive matrix was labelled by the blue reaction product of the Vector SG (Fig. 2D) and was consistently stronger in the ventromedial and caudal axes of the neostriatum. Dehydration in alcohol resulted in leaching of the Vector SG precipitate from labelled structures. This leaching did not occur when the sections were dehydrated using acetone.

Electron microscopic observations

Structures that were positive for BDA were characterized by the typical electron dense DAB

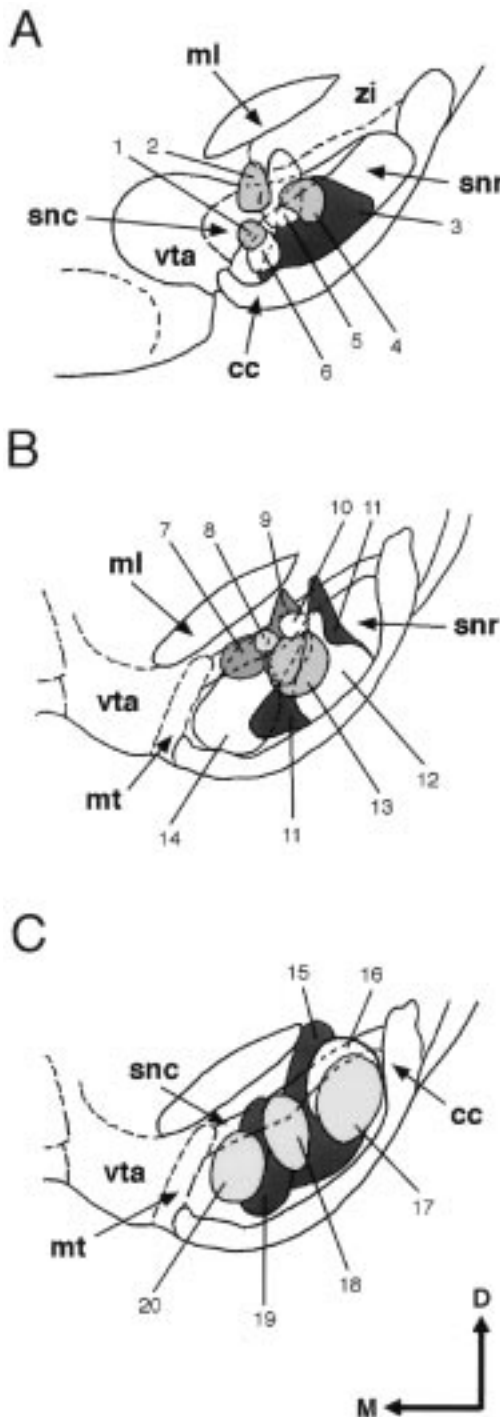
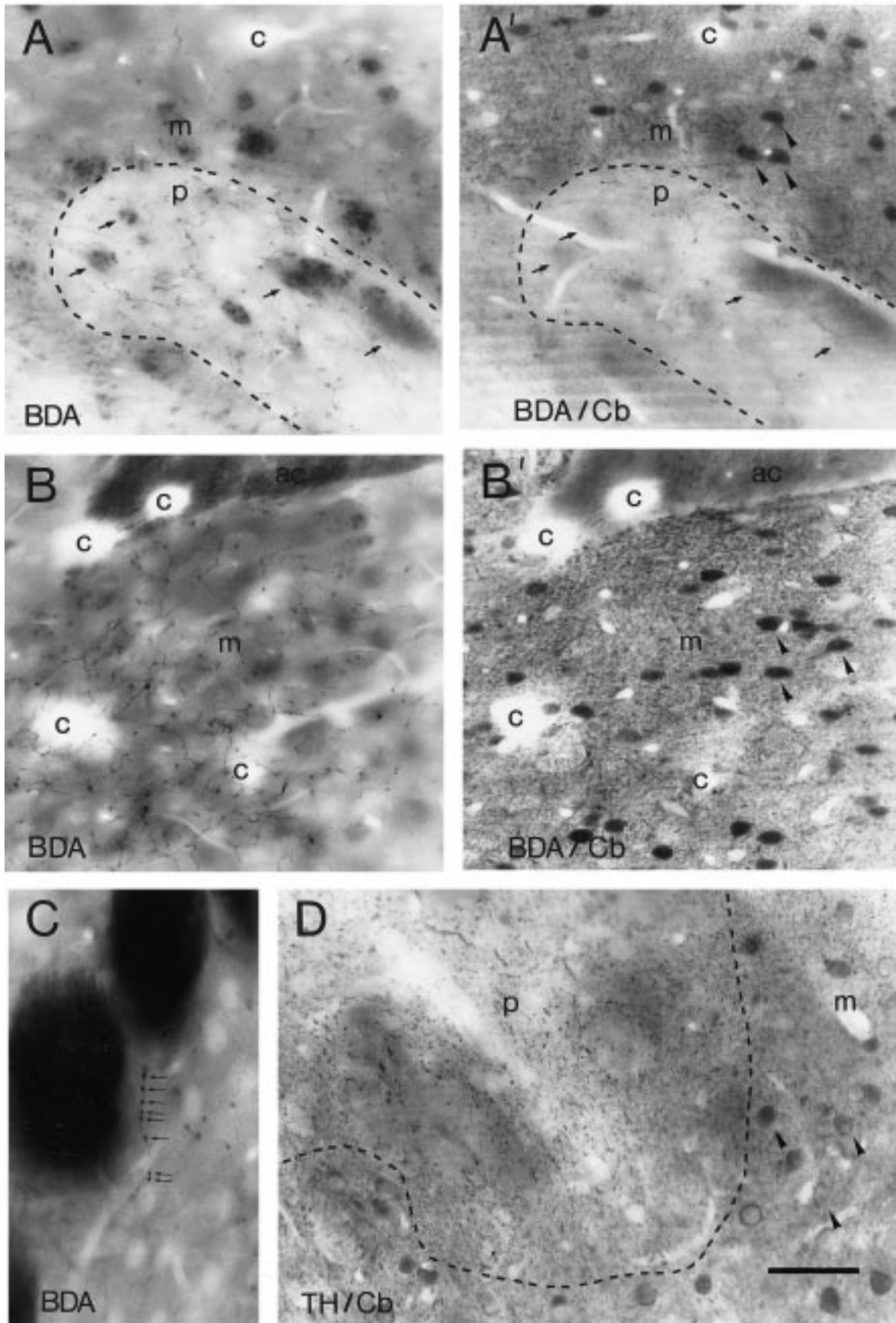


Fig. 1. (A–C) Diagrams of coronal sections through the substantia nigra illustrating the sites of 20 deposits of the anterograde tracer BDA in the substantia nigra. All deposits were at approximately the same rostrocaudal level. Those illustrated in A are at approximately 4.8 mm caudal to the Bregma, those in B and C are at the same rostrocaudal level, approximately 5.2 mm caudal to the Bregma. Injection sizes ranged from 5–10 neurons (e.g., deposit number 1) to the labelling of a large volume of the ventral pars reticulata (snr) (e.g., deposit number 11). All deposits included labelling in the substantia nigra pars compacta (snc) and most also included labelling of the substantia nigra pars reticulata. snc, substantia nigra pars compacta; snr, substantia nigra pars reticulata; ml, medial lemniscus; mt, medial terminal nucleus accessory optic tract; vta, ventral tegmental area; cc, crus cerebri; zi, zona incerta.



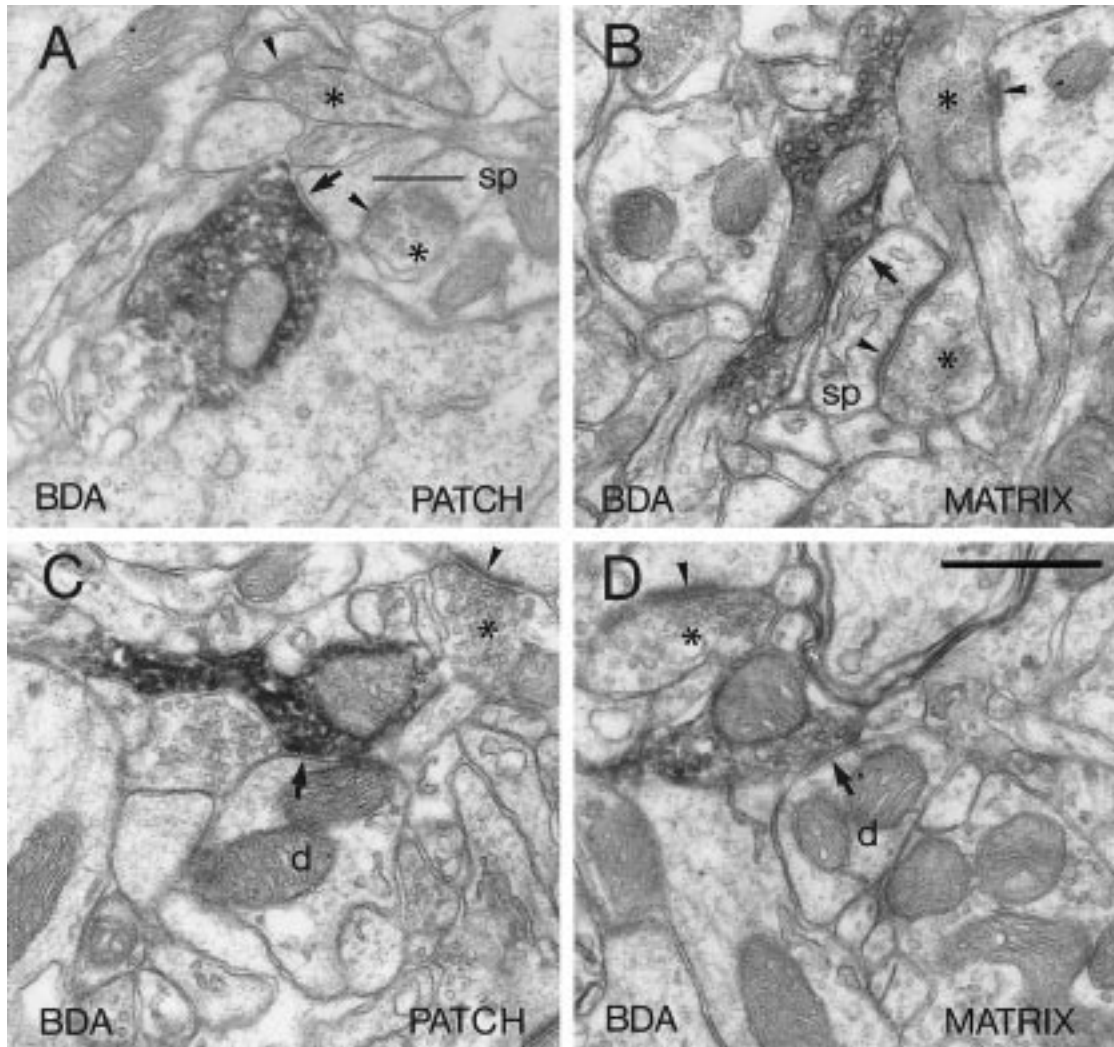


Fig. 3. Electron micrographs illustrating the morphology and synaptology of anterogradely-labelled nigrostriatal boutons in the patch (A and C) and the matrix (B and D). In A and B the anterogradely-labelled boutons form symmetrical synapses (arrows) with dendritic spines (sp) in a patch (A) and the matrix (B). In C and D the anterogradely-labelled boutons form symmetrical synapses (arrows) with dendritic shafts (d) in the patch (C) and the matrix (D). Note the presence of unlabelled terminals (asterisk) forming asymmetrical synapses (arrowheads) with spines. All micrographs are at the same magnification, scale bar in D=0.5 μm.

reaction product which adhered to the outer surfaces of organelles, such as mitochondria, synaptic vesicles, microtubules and the inner surface of the

plasma membrane. The BDA-positive structures included nerve terminals and both myelinated and unmyelinated axons.

Fig. 2. (A, A', B, B') Pairs of light micrographs taken at different focal depths illustrating anterograde labelling (BDA) predominantly confined to a neostriatal patch (p; A, A') and the neostriatal matrix (m; B, B'). The micrographs on the right (A' and B') were taken at the surface of the section where the labelling for calbindin is stronger (some labelled perikarya indicated by arrowheads), those on the left (A and B) were taken deeper in the sections and show the anterograde labelling more clearly. The capillaries (c) and the small arrows indicate landmarks that appear in both micrographs. The broken lines in A and A' indicate the border between the patch and the matrix. Micrographs B and B' were taken from ventral neostriatum, at the level of the anterior commissure (ac), where calbindin labelling is strongest. (C) Micrograph of a Type II anterogradely-labelled axon in the matrix. Small arrows indicate the grape-like varicosities typical of this type of axon. (D) Micrograph of neostriatum double-immunolabelled to reveal both tyrosine hydroxylase and calbindin. This micrograph shows the homogeneous distribution of tyrosine hydroxylase in both the patch (p) and the matrix (m) compartments. The broken line marks the border between the patch and the matrix. Calbindin-positive somata (some illustrated by arrowheads) and dendrites define the matrix. All micrographs are at the same magnification, scale bar in D=50 μm.

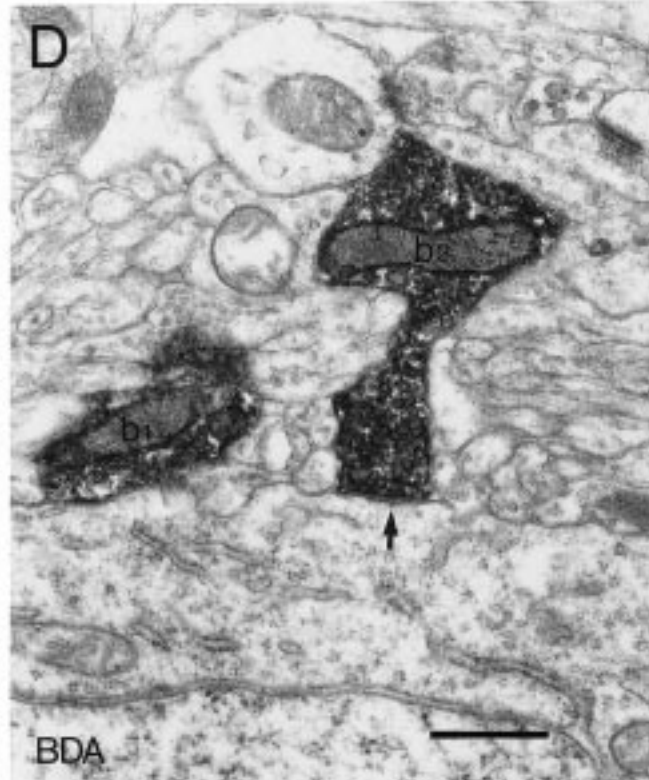
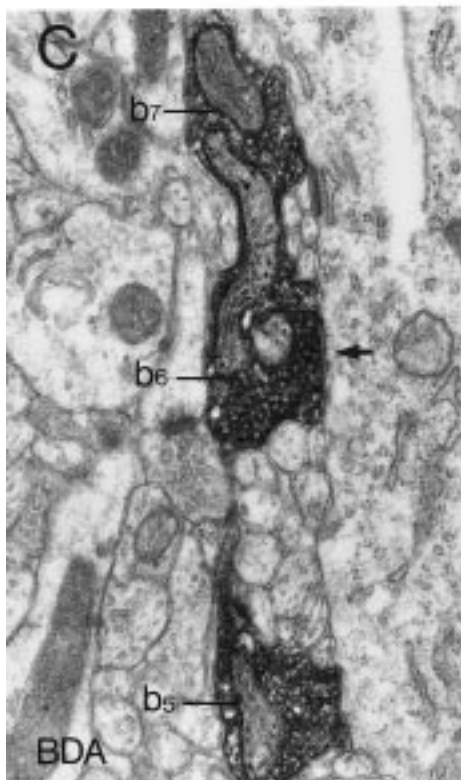
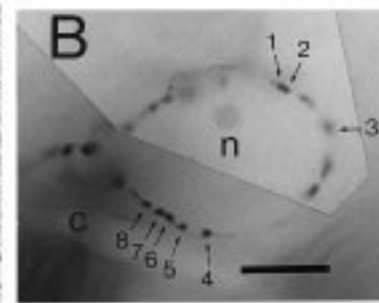
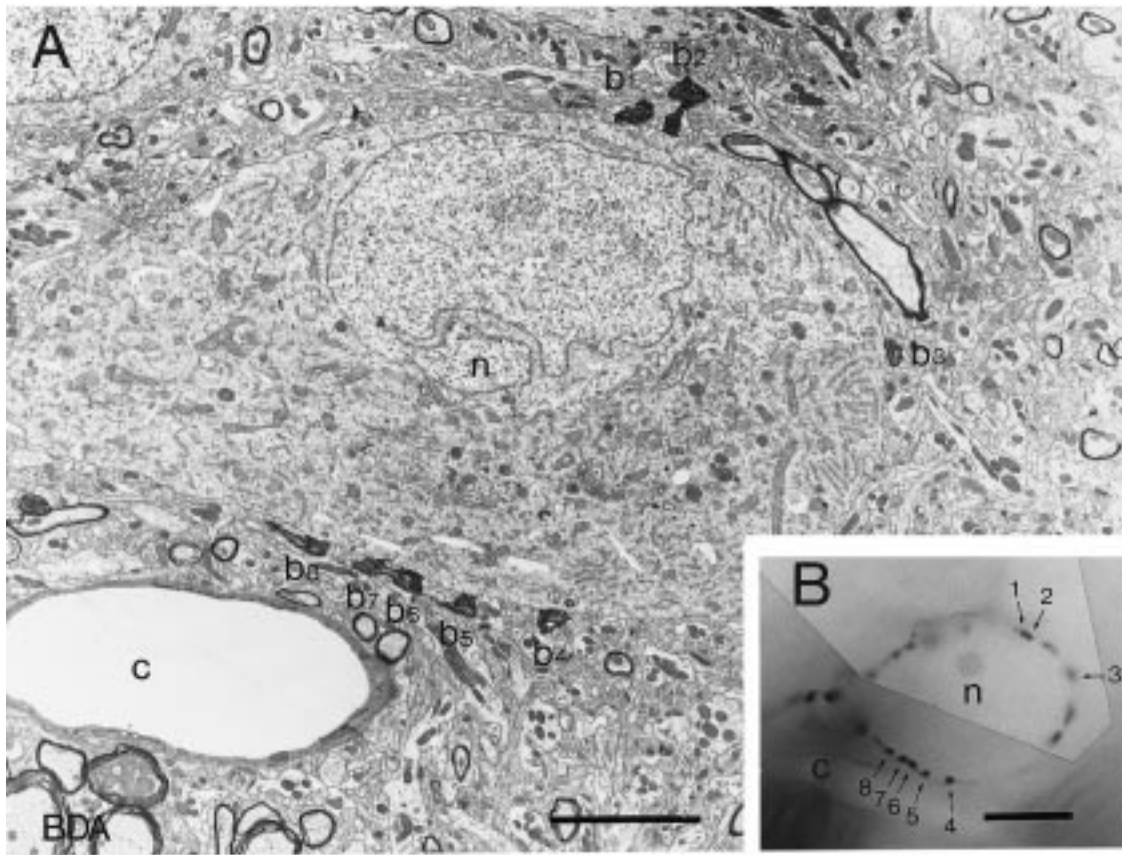


Table 1. The postsynaptic targets of anterogradely-labelled and immunolabelled boutons in the patch and the matrix

Postsynaptic targets	% Tyrosine hydroxylase-positive boutons		% Anterogradely-labelled boutons	
	Patch (128)	Matrix (140)	Patch (72)	Matrix (78)
Spines	42.19 (54)	54.29 (76)	56.94 (41)	60.26 (47)
Dendrites	55.47 (71)	41.43 (58)	41.67 (30)	37.18 (29)
Somata	2.34 (3)	4.29 (6)	1.39 (1)	2.56 (2)

Numbers in parenthesis indicate the number of observations. Chi-squared analysis showed no significant differences between immunopositive boutons in either the patch or the matrix, or between anterogradely-labelled boutons in the patch or the matrix. The ANOVA indicated that there were no significant differences within or between animals. Data obtained from four animals.

Synaptology of anterogradely-labelled Type I axons in the neostriatum. Type I axons formed mainly symmetrical synapses characterized by apposed, parallel membranes separated by a synaptic cleft containing diffuse electron-dense material (Fig. 3). This specialization was associated with a slight thickening of the presynaptic membrane (Fig. 3A), but no postsynaptic thickening. Boutons in both the patches (Fig. 3A,C) and the matrix (Fig. 3B,D) contained many round or pleomorphic vesicles. The boutons made symmetrical synaptic contacts predominantly with spines and dendrites (Fig. 3) and occasionally with somata in both the patches and the matrix. There was no significant difference between the distribution of the postsynaptic targets in the patches and the matrix both within animals and when considered as a population (Table 1). The synapses, which occurred at irregular intervals along the axons, were mainly *en passant* in nature and occurred at small varicosities and at non-varicose parts of the axons. It was thus difficult to define the limits of boutons. An index of the dimension of synaptic boutons was therefore taken as the diameter of the axon perpendicular to the synaptic specialization. The diameter of Type I boutons in the patches was not significantly different from the diameter in the matrix within individual animals nor when all the data were pooled, however the analysis of variance revealed that in one animal the size of boutons in the matrix was significantly smaller ($P=0.012$) than in the other animals (Table 2). Occasionally, BDA-positive terminals forming asymmetrical synapses with dendrites were observed in the matrix ($n=3$).

Synaptology of anterogradely-labelled Type II axons in the neostriatum. Type II boutons were large (cross-sectional area: $0.71 \pm 0.04 \mu\text{m}^2$; $n=112$), usually contained many mitochondria and formed

Table 2. Diameter of immunopositive and anterogradely-labelled terminal boutons in the patch and the matrix

Bouton type	Bouton diameter (μm)	
	Patch	Matrix
Tyrosine hydroxylase-positive	0.307 ± 0.013 ($n=129$) (0.09–0.809)	0.293 ± 0.012 ($n=125$) (0.9–0.684)
Type I anterograde	0.279 ± 0.016 ($n=67$) (0.112–0.663)	0.327 ± 0.018 ($n=77$) (0.124–0.8)
Type II anterograde	–	$0.591 \pm 0.027^\dagger$ ($n=65$) (0.2–1.245)

Data in brackets indicate the number (n) of observations and range. [†]Type II anterogradely-labelled boutons were significantly larger in diameter than tyrosine hydroxylase-positive terminals and Type I anterogradely-labelled terminals in both the patches and the matrix. Type II anterograde boutons were only found in the matrix. The ANOVA indicated that there were no significant differences within or between animals except that in one animal the size of anterogradely-labelled terminals in the matrix were smaller than in the others. Data obtained from six animals for the anterograde and four for the tyrosine hydroxylase immunocytochemistry.

symmetrical synapses with dendrites, spines and perikarya (Fig. 4C,D) and they occasionally exhibited multiple active zones. They were sometimes observed to form varicose pericellular baskets around both medium spiny neurons and neurons showing the ultrastructural characteristics of neostriatal interneurons, i.e. indented nucleus surrounded by a large volume of organelle-rich cytoplasm (Fig. 4A,B). The diameter of Type II boutons was significantly larger than that of both Type I boutons and tyrosine hydroxylase-positive boutons in both patch and matrix (Table 2).

Fig. 4. Correlated light (B) and electron (A) micrographs of a Type II axon outlining the cell body of a large unlabelled neostriatal neuron (n). The indented nucleus and the large expanse of organelle-rich cytoplasm are characteristic of neostriatal interneurons. The boutons indicated by numbers and small arrows are visible in the electron micrograph apposed to the perikaryon (b₁₋₈). A capillary (c) is indicated in both micrographs. (C and D) Higher power electron micrographs of boutons b1, b2 and b5–7, some of which form symmetrical synapses (arrows) with the neostriatal interneuron in this micrograph. Scale bars: A=5 μm ; B=10 μm ; C and D are at the same magnification, bar in D=0.5 μm .

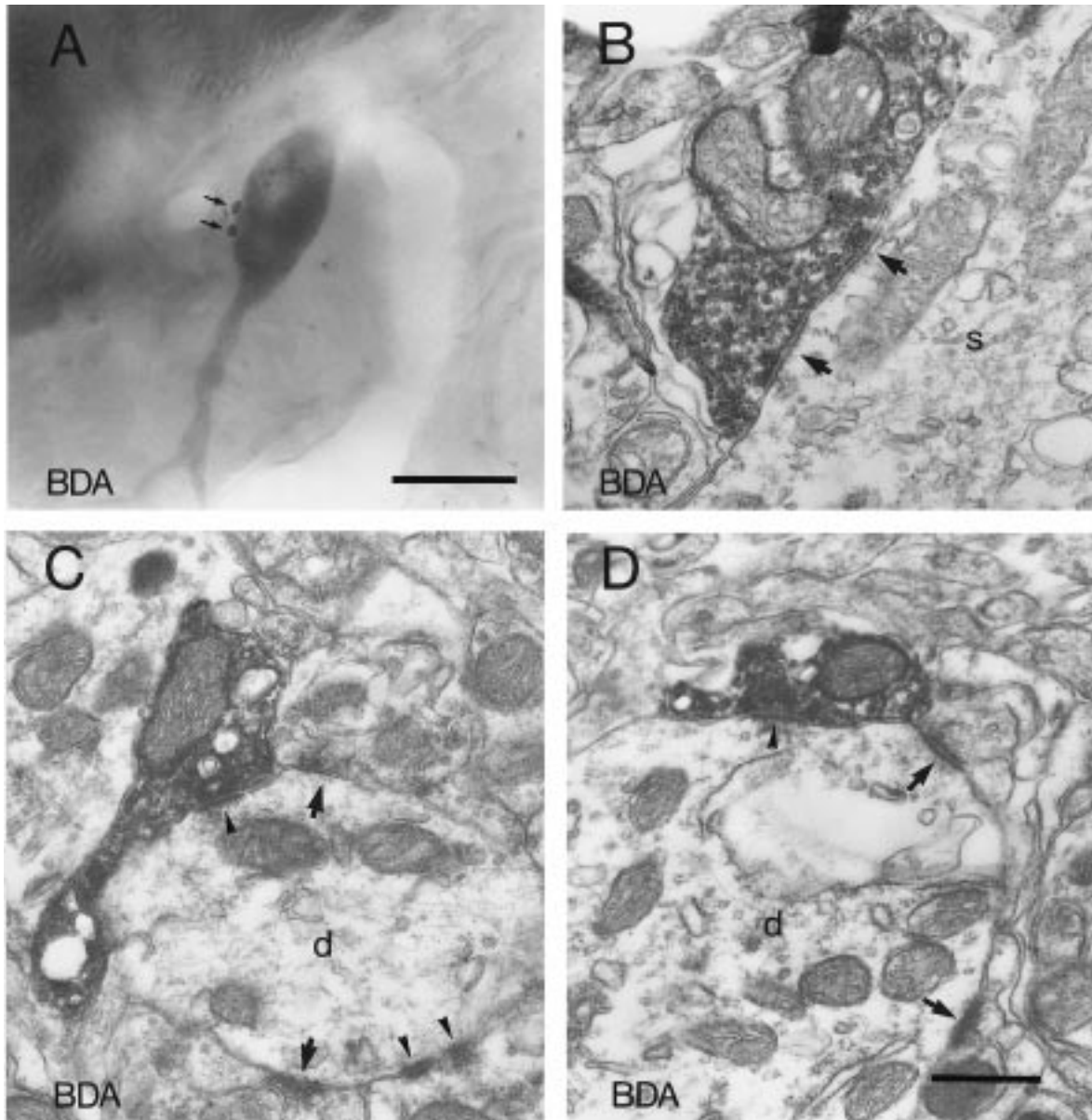


Fig. 5. Light (A) and electron (B–D) micrographs of BDA-positive profiles in the globus pallidus. (A) Light micrograph of a retrogradely-labelled neuron in the globus pallidus with two labelled boutons (small arrows) apposed to the soma. (B) A labelled bouton with pallidal-like morphology forming symmetrical synapses (arrows) with the soma of a pallidal neuron (s). (C and D) Labelled boutons forming asymmetrical synapses (arrowheads) with pallidal dendrites (d) which also receive inputs from unlabelled boutons forming either asymmetrical (arrowheads) or symmetrical (arrows) synapses. Scale bars: A=20 μm ; B–D are at the same magnification, bar in D=0.5 μm .

As the electron microscopic analysis of Type II boutons was carried out by correlated light and electron microscopy i.e. the axons were first selected at the light microscopic level and then examined by electron microscopy, the sample is non-random. We therefore cannot comment on the distribution of postsynaptic targets. However, in the analysis of Type II axons that were not identified as forming pericellular baskets, it was evident that the majority

(73.5%) made synaptic contact with dendritic shafts and only 17.6% were in contact with spines.

Synaptology of biotinylated dextran amine-labelled boutons within the globus pallidus. Boutons within the globus pallidus labelled with BDA were of two types. The first were large boutons with irregular outlines, containing many mitochondria and formed symmetrical, axosomatic synapses that often exhibited

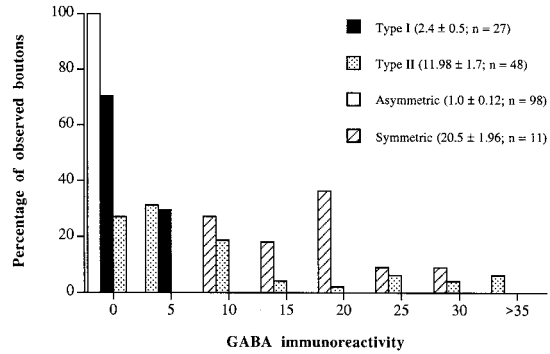
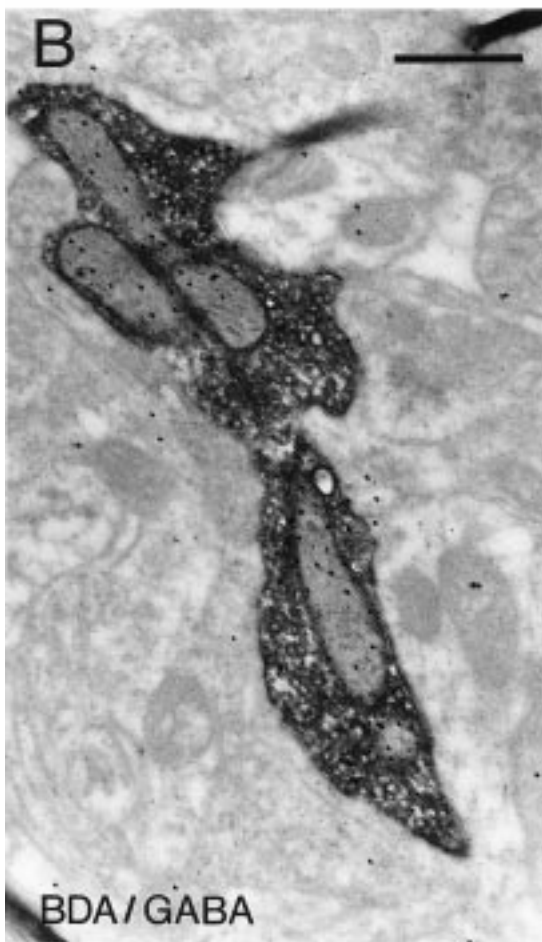
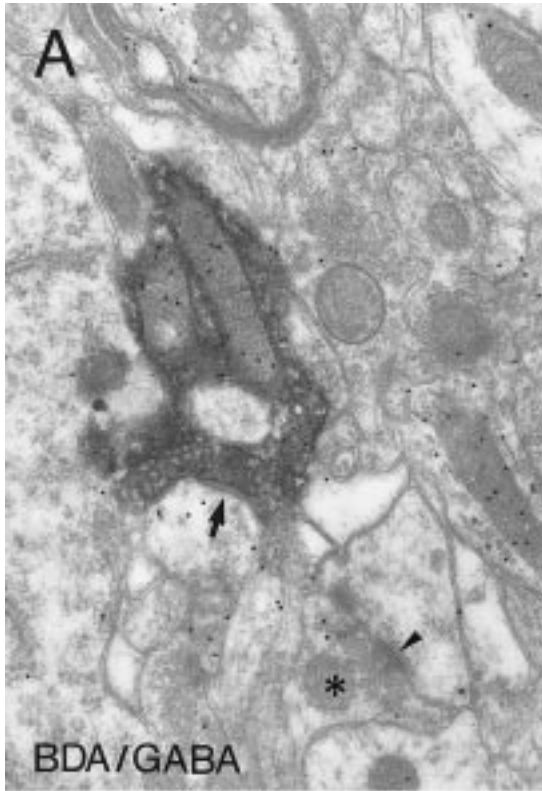
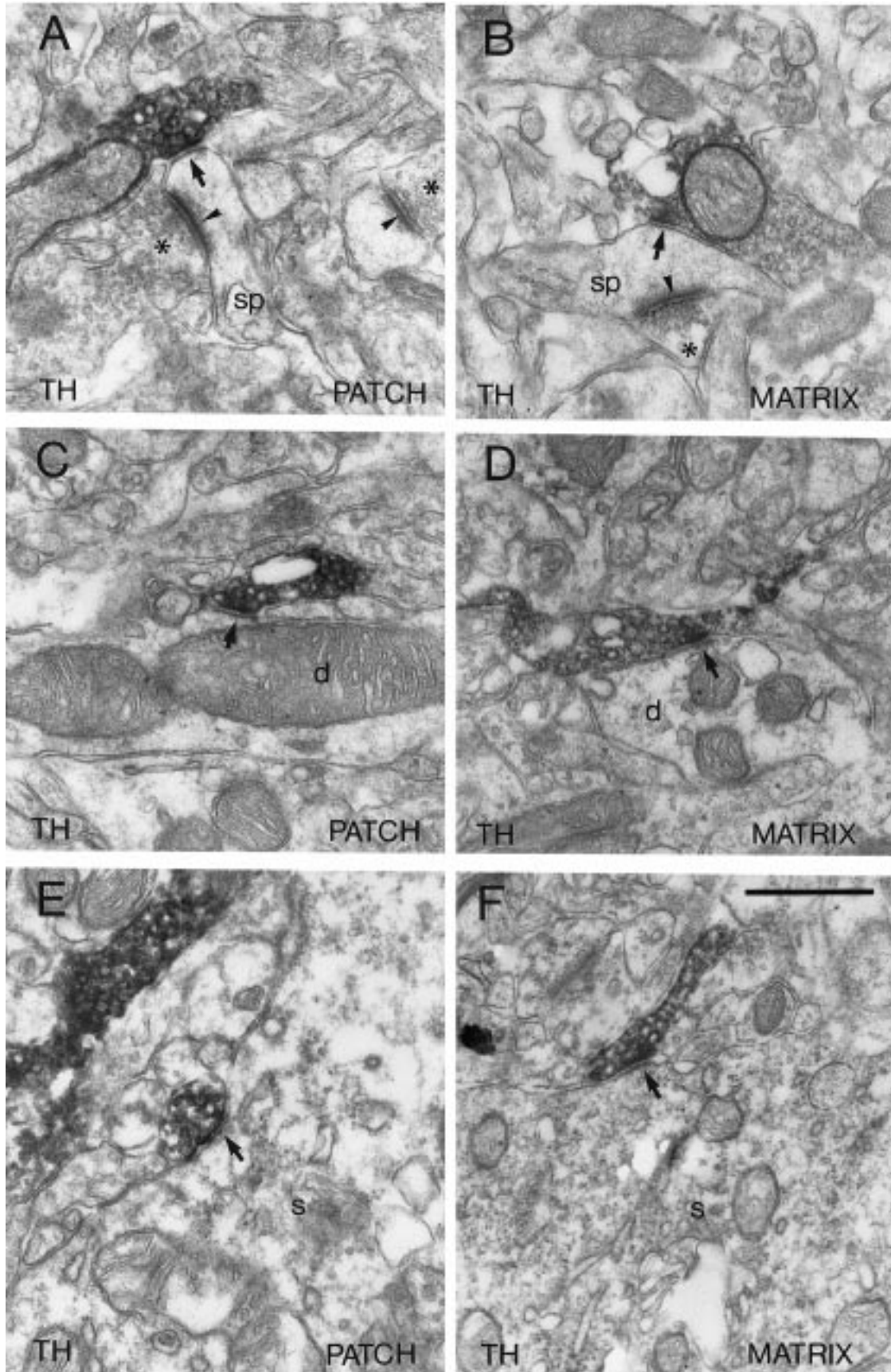


Fig. 7. Frequency distribution of the levels of GABA immunoreactivity in anterogradely-labelled and unlabelled terminals in the neostriatum. Type I and Type II refer to anterogradely-labelled terminals; Asymmetric refers to unlabelled terminals forming asymmetric synapses; Symmetric refers to unlabelled terminals forming symmetrical synapses. Figures in brackets are the mean \pm S.E.M. and the number of boutons. Type II anterogradely-labelled terminals had a significantly higher index of GABA immunoreactivity than either Type I anterogradely-labelled terminals or terminals forming asymmetrical synapses i.e. putative glutamatergic terminals. In contrast, the index of immunoreactivity in Type I anterogradely labelled terminals was not significantly different to terminals forming asymmetrical synapses. All indices of immunoreactivity were significantly lower than those found in terminals forming symmetrical synapses i.e. putative GABAergic terminals.

multiple active zones (cross-sectional area: $0.63 \pm 0.1 \mu\text{m}^2$; $n=6$; Fig. 5B). A second type of BDA-positive terminals within the globus pallidus was observed forming asymmetrical synapses with dendrites (cross-sectional area: $0.39 \pm 0.03 \mu\text{m}^2$; $n=5$; Fig. 5C,D) and somata (cross-sectional area: $0.42 \pm 0.1 \mu\text{m}^2$; $n=3$) (not shown).

Post-embedding GABA immunolabelling of anterogradely labelled nigrostriatal axons. Regions of neostriatum rich in either anterogradely-labelled Type I or Type II axons were selected, re-embedded, sectioned and immunolabelled for GABA by the post-embedding technique (Fig. 6). Immunolabelling for GABA was strong over the majority of terminals forming symmetrical synapses and some myelinated axons. It was low over terminals forming asymmetrical synapses, some myelinated axons and all somata that were observed. The quantitative analysis revealed that Type II anterogradely-labelled

Fig. 6. (A,B) Electron micrographs of BDA-labelled Type II boutons in the neostriatum which have been processed by the immunogold method to reveal GABA-immunoreactivity. The labelled bouton A is in symmetrical synaptic contact (arrow) with an unlabelled profile. This bouton was found to have an index of GABA-immunoreactivity of 2.51. The labelled bouton in B, which is not synaptic at this level, had an index of GABA-immunoreactivity of 7.15. Note the unlabelled bouton in A (asterisk) which forms an asymmetrical synapse (arrow-head) and is GABA-negative. Bar in B = 0.5 μm .



axons were significantly enriched in GABA-immunoreactivity (Fig. 7) compared to that associated with boutons forming asymmetrical synapses i.e. putative glutamatergic boutons (Fig. 7). Similarly, Type I anterogradely-labelled axons (Fig. 7) had significantly lower levels of GABA-immunoreactivity than boutons forming symmetric synapses but levels similar to those found in boutons forming asymmetrical synapses (Fig. 7).

Synaptology of tyrosine hydroxylase-positive axons in the neostriatum. Tyrosine hydroxylase-positive axons were of small diameter and contained round or pleomorphic vesicles. They gave rise to varicosities that contained densely packed vesicles and mitochondria (Fig. 8). They formed symmetrical synapses predominantly with spines and dendrites and occasionally with somata in both the patch and matrix (Fig. 8). As was the case with Type I anterogradely-labelled boutons, synapses occurred at both varicose and non-varicose sections of the labelled axon. The distribution of structures postsynaptic to the immunolabelled boutons was not significantly different in the patch and matrix (Table 1). The diameter of immunolabelled synaptic boutons in the patches was not significantly different from that of the matrix (Table 2) nor were they significantly different from anterogradely labelled Type I axons. Occasionally, immunopositive terminals forming asymmetrical synapses were observed in patches (dendrites; $n=2$) and the matrix (spines; $n=1$).

DISCUSSION

The main findings of the present study confirm and extend our knowledge of the synaptology of the nigrostriatal projection in the rat. The electron microscopic analysis of tyrosine hydroxylase immunolabelled profiles confirmed previous findings that dopaminergic terminals in the neostriatum form symmetrical synapses with spines and dendrites, and to a lesser extent with somata. The present study shows for the first time at the electron microscopic level that the majority of anterogradely-labelled nigrostriatal terminals were indistinguishable from tyrosine hydroxylase-immunopositive terminals in terms of their size, morphology, type of synaptic specialization and distribution of postsynaptic targets. In confirmation of previous findings,³¹ the anterograde labelling revealed a second, rarer type of axon in the neostriatum that becomes labelled by anterograde tracer placed in the substantia nigra. Our electron

microscopic study however, demonstrated that these axons have a different morphology to the majority of anterogradely-labelled and tyrosine hydroxylase-immunolabelled terminals, that they are GABA-immunopositive and are thus not likely to be dopaminergic axons. The major new findings of the present study are that nigrostriatal terminals identified by either tyrosine hydroxylase immunocytochemistry or by anterograde labelling from the substantia nigra are of similar dimensions, form similar types of synapses and have a similar distribution of postsynaptic targets in both the patch and matrix compartments of the neostriatum. These findings lead to the conclusion that the anatomical substrate for the modulation of cortical information flow through the basal ganglia by the dopaminergic input from the substantia nigra is similar in the patch and matrix compartments of the neostriatum.

Technical considerations

In order to address the question of possible differences in synaptology between patch and matrix compartments of the neostriatum, it was necessary to use double labelling techniques and to analyse the results at the electron microscopic level. Technical issues relating to the use of double peroxidase techniques have been discussed extensively on previous occasions.^{9,58,72} In the present experiments, the possibility of cross reaction was kept to a minimum by the use of the avidin-biotin-peroxidase technique for one chromogen and peroxidase-antiperoxidase for the other. Furthermore, the omission of either one of the primary antibodies in the double immunocytochemical experiments or omission of the ABC in the anterograde studies resulted in labelling by one chromogen only, indicating that there was no cross reaction between the procedures. The blind electron microscopic analysis of these control preparations by separate investigators demonstrated that the reaction product formed by the DAB is distinguishable from that formed by the Vector SG and also indicated that the two reaction products do not interact appreciably.

Although immunoreactivity for calbindin is one of the most reliable markers for the patch-matrix complex across different species³⁰ and readily lends itself to double-labelling procedures, the labelling is heterogeneous such that the ventral and medial regions of the neostriatum are strongly labelled whereas there is little or no immunolabelling of the dorsal neostriatum. Our data relating to the

Fig. 8. Electron micrographs illustrating the morphology and synaptology of tyrosine hydroxylase-immunolabelled boutons in the patch (A, C and E) and the matrix (B, D and F). These micrographs show tyrosine hydroxylase-positive boutons forming symmetrical synapses (arrows) with dendritic spines (sp; A and B), dendritic shafts (d; C and D) and somata (s; E and F) in the patch and the matrix. Note the presence of unlabelled terminals (asterisk) in A and B forming asymmetrical synapses (arrowheads) with spines. All micrographs are at the same magnification, scale bar in F=0.5 μ m.

Table 3. Percentage distribution of dopaminergic axons to postsynaptic targets in the neostriatum

Postsynaptic targets	Present study \diamond	Freund <i>et al.</i> [†]	Zahm ^{††}	Groves <i>et al.</i> [*]	Descarries <i>et al.</i> [△]
Spines	51.10	56.5	65	56	30
Dendritic shafts	45.79	36.2	30	42	67
Somata	3.16	6.1	2	2	3

\diamond Combined mean of Type I anterograde and tyrosine hydroxylase-immunopositive data.

[†]All TH-immunoreactive profiles observed in the neostriatum.

^{††}Estimated from histogram of presented data.

^{*}Data from 5-hydroxydopamine-labelled axons.

[△]Combined immunocytochemical and autoradiographic data.

patch-matrix are thus derived from the ventral two-thirds of the neostriatum and may not necessarily apply to its whole dorsoventral extent.

While the presence of glutaraldehyde in the fixing medium is necessary to ensure the adequate preservation of the ultrastructure to allow electron microscopic analysis, it causes a shrinkage of the brain tissue which may not be linearly related to the size of the structures nor to the concentration of glutaraldehyde. It is possible that measurements made relating to the linear size of structures in different animals may be affected by the concentration of glutaraldehyde. The statistical comparison of data from individual animals using both the Mann-Whitney *U*-test and the Kruskal-Wallis ANOVA showed that there was no significant difference in the diameter or distribution of anterogradely- or immunocytochemically-labelled axons in the patch and the matrix of the same animal or between animals in the same experimental group. However, in one case the terminals were significantly smaller in the matrix when compared to the other animals. The reason for the latter observation is unknown, but it does not affect the central finding that there were no differences between patch and matrix.

Nigrostriatal projection visualized by anterograde labelling and immunocytochemistry

In order to characterize the projection from the substantia nigra to the different compartments of the neostriatum we used two approaches, immunocytochemistry for tyrosine hydroxylase and anterograde labelling from the substantia nigra. Although immunocytochemistry for tyrosine hydroxylase will label all structures that synthesize catecholamines, it is well established that in the neostriatum, most tyrosine hydroxylase is associated with dopaminergic structures. The ultrastructural morphology of the terminals labelled by the anterograde labelling (Type I) or by immunocytochemistry for tyrosine hydroxylase, their dimensions, the type of synaptic specialization that they formed and the distribution of the postsynaptic targets were very similar. It is thus likely that Type I anterogradely-labelled terminals and tyrosine hydroxylase-positive terminals are from the

same population of neurons that form the dopaminergic nigrostriatal projection. Furthermore, the distribution of postsynaptic targets is similar to that observed in most of the previous ultrastructural analyses of dopaminergic terminals in the neostriatum labelled by different methods (Table 3).

At the light microscopic level the density of tyrosine hydroxylase staining was homogeneous, there was no apparent differences between patches and the matrix identified on the basis of calbindin immunocytochemistry. Similarly, Type I anterogradely-labelled fibres were observed in both patches and the matrix. At the electron microscopic level, it was also clear that there were similarities between the innervation of the patches and matrix by axons labelled by anterograde tracing or by tyrosine hydroxylase immunocytochemistry. They formed the same type of synaptic specializations with the same postsynaptic targets and there was no statistical difference between the sizes of their terminals and their distribution to postsynaptic targets in the patches and matrix (Tables 1, 2). Thus, despite the fact that the dopaminergic innervation of the patch and matrix arises from different populations of dopamine neurons in the ventral mesencephalon^{31,46} that are neurochemically distinct^{25,31,57,83} and show structural differences,^{48,54,75} the morphology of their axons and terminals in the neostriatum are similar, as is the pattern of innervation of neurons in the patch and matrix.

One of the roles of the dopaminergic input to the neostriatum is to modulate the flow of cortical information through the basal ganglia by making direct synaptic contact with the spiny output neurons that receive the major part of the cortical input to the neostriatum.^{29,36} Our results demonstrate that the anatomical substrate for this type of modulatory role, and thus the mechanism, is likely to be similar in both striatal compartments.

Type II axons and boutons

In addition to the Type I anterogradely-labelled fibres, we also observed a second, rarer class of labelled axon (Type II) that was morphologically and neurochemically distinct. Whereas the Type I axons

probably correspond to classes A and B described by Gerfen *et al.*,³¹ the Type II probably corresponds to the class C of Gerfen *et al.*³¹ which were identified as non-dopaminergic. Our observations also suggest that this class of axons is non-dopaminergic. First, they were not observed in the tissue that was immunostained to reveal tyrosine hydroxylase and have not been described in previous immunocytochemical or histochemical studies of the neostriatum.^{3,19,24,40,65,85} Secondly, they display immunoreactivity for GABA. These axons are thus not part of the dopaminergic nigrostriatal projection. There are two possible sources of these Type II axons. 1) They may represent the axons of the non-dopaminergic nigrostriatal projection which has been proposed to account for 5% of nigrostriatal neurons.^{31,42,76} 2) Alternatively, or additionally, at least some of the Type II axons may be derived from the globus pallidus. Evidence in favour of this is the morphology and synaptic specialization of Type II axons and boutons are similar to those of pallidal terminals and, like pallidal terminals, they are GABA-positive.^{11,12,71,72} Furthermore, Type II axons and boutons were only observed in animals in which retrograde labelling occurred in the globus pallidus; they may have become labelled by retrograde transport to somata and then anterograde transport along axon collaterals. This kind of multimodal transport is known to occur commonly in the basal ganglia.⁶⁹ The exact origin of these axons remains to be established.

Anterogradely-labelled axons were commonly observed coursing through the globus pallidus which presumably represent nigrostriatal axons. Axons giving rise to boutons that formed either symmetrical and asymmetrical synapses were also observed. These axons presumably represent the nigropallidal projection that has been previously described,^{61,84} but may also include the axon collaterals of retrogradely-labelled pallidal neurons or the collaterals of other neurons that may have transported the BDA both retrogradely and anterogradely e.g., neurons of the subthalamic nucleus.

CONCLUSIONS

The patch-matrix organization of the striatal complex has been proposed to reflect the mechanisms of

information processing in allocortical and neocortical regions.³² Thus the connections of patches are analogous to those of allocortical areas and receive input preferentially from cortical neurons that have allocortical connective features, whereas the connections of the matrix are analogous to those of neocortical areas and receive input preferentially from cortical neurons that have neocortical connective features.³² Of critical importance in this organization is the feedback projection from the midbrain dopamine neurons to the neostriatum. As indicated earlier, the nigrostriatal input to the patches and matrix originates from distinct populations of dopamine neurons; the present study shows that the synaptology of these afferents is similar in the patches and the matrix located in the ventral two-thirds of the neostriatum. This suggests that, at least in relation to the dopaminergic innervation, the mechanism or anatomical substrate for the modulation of different cortical information carried by corticostriatal neurons selectively innervating patch or matrix, is essentially the same.

The findings of the present study raise a number of questions. Although there are apparent differences in the dopaminergic innervation of the patches and the matrix, it remains to be established whether the other afferents that show selectivity in the innervation of the patches and the matrix have a similar synaptology in both compartments. Furthermore, it remains to be established whether the innervation of neurons in the patches and the matrix by neostriatal interneurons, whose axons selectively arborize in the matrix, is quantitatively and/or qualitatively different in the two compartments.^{15,26,37,49,50,55} The answers to these questions will help in our understanding of whether the essential operations performed by neurons in the neostriatum is the same in the patch and the matrix compartments and whether differences between the patch and matrix relate only to the differences in their afferent and/or efferent connections.

Acknowledgements—The authors thank Caroline Francis, Liz Norman, Paul Jays and Frank Kennedy for technical assistance. We also thank Peter Somogyi for the GABA antiserum and Nick Clarke for comments on the manuscript. This work was funded by the Medical Research Council, U.K. J.J.H. is in receipt of an MRC Research Studentship.

REFERENCES

1. Albin R. L., Young A. B. and Penney J. B. (1989) The functional anatomy of basal ganglia disorders. *Trends Neurosci.* **12**, 366–375.
2. Alexander G. E., Crutcher M. D. and DeLong M. R. (1990) Basal ganglia-thalamocortical circuits: parallel substrates for motor, oculomotor, "prefrontal" and "limbic" functions. *Prog. Brain Res.* **85**, 119–146.
3. Arluison M., Dietl M. and Thibault J. (1984) Ultrastructural morphology of dopaminergic nerve terminals and synapses in the striatum of the rat using tyrosine hydroxylase immunocytochemistry: a topographical study. *Brain Res. Bull.* **13**, 269–285.
4. Beckstead R. M. (1985) Complementary mosaic distribution of thalamic and nigral axons in the caudate nucleus of the cat: double anterograde labelling combining autoradiography and wheat germ-HRP histochemistry. *Brain Res.* **335**, 153–159.

5. Beckstead R. M., Domesick V. B. and Nauta W. J. H. (1979) Efferent connections of the substantia nigra and ventral tegmental area in the rat. *Brain Res.* **175**, 191–217.
6. Bennett B. D. and Bolam J. P. (1994) Localisation of parvalbumin-immunoreactive structures in primate caudate-putamen. *J. comp. Neurol.* **347**, 340–356.
7. Berendse H. W., de Galis G. Y. and Groenewegen H. J. (1992) Topographical organization and relationship with ventral striatal compartments of prefrontal corticostriatal projections in the rat. *J. comp. Neurol.* **316**, 314–347.
8. Bevan M. D., Francis C. M. and Bolam J. P. (1995) The glutamate-enriched cortical and thalamic input to neurons in the subthalamic nucleus of the rat: convergence with GABA-positive terminals. *J. comp. Neurol.* **361**, 491–511.
9. Bolam J. P. and Ingham C. A. (1990) Combined morphological and histochemical techniques for the study of neuronal microcircuits. In *Handbook of Chemical Neuroanatomy* (eds Björklund A., Hökfelt T., Wouterlood F. and van den Pol A.), Vol. 8, pp. 125–198. Elsevier Biomedical Publications, Amsterdam.
10. Bolam J. P., Izzo P. N. and Graybiel A. M. (1988) Cellular substrate of the histochemically-defined striosome/matrix system of the caudate nucleus: a combined Golgi and immunocytochemical study in the cat and ferret. *Neuroscience* **24**, 853–875.
11. Bolam J. P. and Smith Y. (1992) The striatum and the globus pallidus send convergent synaptic inputs onto single cells in the entopeduncular nucleus of the rat: a double anterograde labeling study combined with post-embedding immunocytochemistry for GABA. *J. comp. Neurol.* **321**, 456–476.
12. Bolam J. P., Smith Y., Ingham C. A., von Krosigk M. and Smith A. D. (1993) Convergence of synaptic terminals from the striatum and the globus pallidus onto single neurones in the substantia nigra and the entopeduncular nucleus. In *Progress in Brain Research* (eds Arbuthnott G. W. and Emson P. C.), Vol. 99, pp. 73–88. Elsevier Science Publishers, Amsterdam.
13. Brodal P. (1992) The Basal Ganglia. In *The Central nervous System: Structure and Function*, pp. 246–261. Oxford University Press, New York.
14. Chesselet M.-F. and Delfs J. M. (1996) Basal ganglia and movement disorders: an update. *Trends Neurosci.* **19**, 417–422.
15. Chesselet M. F. and Graybiel A. M. (1986) Striatal neurons expressing somatostatin-like immunoreactivity: evidence for a peptidergic interneuronal system in the cat. *Neuroscience* **17**, 547–571.
16. DeLong M. R. (1990) Primate models of movement disorders of basal ganglia origin. *Trends Neurosci.* **13**, 281–285.
17. DeLong M. R., Alexander G. E., Georgopoulos A. P., Crutcher M. D., Mitchell S. J. and Richardson R. T. (1984) Role of the basal ganglia in limb movements. *Human Neurobiol.* **2**, 235–244.
18. DeLong M. R., Alexander G. E., Mitchell S. J. and Richardson R. T. (1986) The contribution of basal ganglia to limb control. *Prog. Brain Res.* **64**, 161–174.
19. Descarries L., Watkins K. C., Garcia S., Bosler O. and Doucet G. (1996) Dual character, asynaptic and synaptic, of the dopamine innervation in adult rat neostriatum: A quantitative autoradiographic and immunocytochemical analysis. *J. comp. Neurol.* **375**, 167–186.
20. DiFiglia M., Christakos S. and Aronin N. (1989) Ultrastructural localization of immunoreactive calbindin-D28k in the rat and monkey basal ganglia, including subcellular distribution with colloidal gold labeling. *J. comp. Neurol.* **279**, 653–665.
21. Donoghue J. P. and Herkenham M. (1986) Neostriatal projections from individual cortical fields conform to histochemically distinct striatal compartments in the rat. *Brain Res.* **397**, 397–403.
22. Eblen F. and Graybiel A. M. (1995) Highly restricted origin of prefrontal cortical inputs to striosomes in the Macaque monkey. *J. Neurosci.* **15**, 5999–6013.
23. Fallon J. H. and Moore R. Y. (1978) Catecholamine innervation of the basal forebrain. 4. Topography of the dopamine projection to the basal forebrain and neostriatum. *J. comp. Neurol.* **180**, 545–580.
24. Freund T. F., Powell J. F. and Smith A. D. (1984) Tyrosine hydroxylase-immunoreactive boutons in synaptic contact with identified striatonigral neurons, with particular reference to dendritic spines. *Neuroscience* **13**, 1189–1215.
25. Gaspar P., Heizmann C. W. and Kaas J. H. (1993) Calbindin D-28K in the dopaminergic mesocortical projection of a monkey (*Aotus trivirgatus*). *Brain Res.* **603**, 166–172.
26. Gerfen C. R. (1984) The neostriatal mosaic: compartmentalization of corticostriatal input and striatonigral output systems. *Nature* **311**, 461–464.
27. Gerfen C. R. (1985) The neostriatal mosaic I: Compartmental organization of projections from the striatum to the substantia nigra in the rat. *J. comp. Neurol.* **236**, 454–476.
28. Gerfen C. R. (1989) The neostriatal mosaic: striatal patch-matrix organization is related to cortical lamination. *Science* **246**, 385–388.
29. Gerfen C. R. (1992) The neostriatal mosaic: multiple levels of compartmental organization in the basal ganglia. *A. Rev. Neurosci.* **15**, 285–320.
30. Gerfen C. R., Baimbridge K. G. and Miller J. J. (1985) The neostriatal mosaic: Compartmental distribution of calcium-binding protein and parvalbumin in the basal ganglia of the rat and monkey. *Proc. natn. Acad. Sci. U.S.A.* **82**, 8780–8784.
31. Gerfen C. R., Herkenham M. and Thibault J. (1987) The neostriatal mosaic: II. Patch- and matrix-directed mesostriatal dopaminergic and non-dopaminergic systems. *J. Neurosci.* **7**, 3915–3934.
32. Gerfen C. R. and Wilson C. J. (1996) The basal ganglia. In *Handbook of Chemical Neuroanatomy* (eds Swanson L. W., Björklund A. and Hökfelt T.), Vol. 12, pp. 371–468. Elsevier Science, Amsterdam.
33. Graybiel A. M. (1990) The basal ganglia and the initiation of movement. *Rev. Neurol.* **146**, 570–574.
34. Graybiel A. M. (1990) Neurotransmitters and neuromodulators in the basal ganglia. *Trends Neurosci.* **13**, 244–254.
35. Graybiel A. M. (1995) Building action repertoires: memory and learning functions of the basal ganglia. *Curr. Opin. Neurobiol.* **5**, 733–741.
36. Graybiel A. M., Aosaki T., Flaherty A. W. and Kimura M. (1994) The basal ganglia and adaptive motor control. *Science* **265**, 1826–1931.
37. Graybiel A. M., Baughman R. W. and Eckenstein F. (1986) Cholinergic neuropil of the striatum observes striosomal boundaries. *Nature* **323**, 625–627.
38. Graybiel A. M., Ragsdale C. W. and Moon Edley S. (1979) Compartments in the striatum of the cat observed by retrograde cell labeling. *Expl Brain Res.* **34**, 189–195.

39. Graybiel A. M. and Ragsdale C. W. J. (1978) Histochemically distinct compartments in the striatum of human, monkey, and cat demonstrated by acetylcholinesterase staining. *Proc. natn. Acad. Sci. U.S.A.* **75**, 5723–5726.
40. Groves P. M., Linder J. C. and Young S. J. (1994) 5-Hydroxydopamine-labeled dopaminergic axons: three-dimensional reconstructions of axons, synapses and postsynaptic targets in rat neostriatum. *Neuroscience* **58**, 593–604.
41. Groves P. M., Martone M., Young S. J. and Armstrong D. M. (1988) Three-dimensional pattern of enkephalin-like immunoreactivity in the caudate nucleus of the cat. *J. Neurosci.* **8**, 892–900.
42. Guyenet P. G. and Crane J. K. (1981) Non-dopaminergic nigrostriatal pathway. *Brain Res.* **213**, 291.
43. Heimer L., Zahm D. S. and Alheid G. F. (1995) Basal Ganglia. In *The Rat Nervous System* (ed G. Paxinos), pp. 579–628. Academic Press Inc., New York.
44. Herkenham M. and Pert C. B. (1981) Mosaic distribution of opiate receptors, parafascicular projections and acetylcholinesterase in rat striatum. *Nature* **291**, 415–418.
45. Hodgson A. J., Penke B., Erdei A., Chubb I. W. and Somogyi P. (1985) Antisera to γ -aminobutyric acid. I. Production and characterization using a new model system. *J. Histochem. Cytochem.* **33**, 229–239.
46. Jimenez-Castellanos J. and Graybiel A. M. (1987) Subdivisions of the dopamine-containing A8-A9-A10 complex identified by their differential mesostriatal innervation of striosomes and extrastriosomal matrix. *Neuroscience* **23**, 223–242.
47. Johnston J. G., Gerfen C. R., Haber S. N. and van der Kooy D. (1990) Mechanisms of striatal pattern formation: conservation of mammalian compartmentalization. *Devl Brain Res.* **57**, 93–102.
48. Juraska J. M., Wilson C. J. and Groves P. M. (1977) The substantia nigra of the rat. A Golgi study. *J. comp. Neurol.* **172**, 585–600.
49. Kawaguchi Y. (1992) Large aspiny cells in the matrix of the rat neostriatum *in vitro*: physiological identification, relation to the compartments and excitatory postsynaptic currents. *J. Neurophysiol.* **67**, 1669–1683.
50. Kawaguchi Y., Wilson C. J., Augood J. and Emson P. C. (1995) Striatal interneurons: chemical, physiological and morphological characterization. *Trends Neurosci.* **18**, 527–535.
51. Kawaguchi Y., Wilson C. J. and Emson P. C. (1989) Intracellular recording of identified neostriatal patch and matrix spiny cells in a slice preparation preserving cortical inputs. *J. Neurophysiol.* **62**, 1052–1068.
52. Kawaguchi Y., Wilson C. J. and Emson P. C. (1990) Projection subtypes of rat neostriatal matrix cells revealed by intracellular injection of biocytin. *J. Neurosci.* **10**, 3421–3438.
53. Kemp J. M. and Powell T. P. S. (1971) The structure of the caudate nucleus of the cat: light and electron microscopy. *Phil. Trans. R. Soc. B* **262**, 383–401.
54. Kita T., Kita H. and Kitai S. T. (1986) Electrical membrane properties of rat substantia nigra compacta neurons in an *in vitro* slice preparation. *Brain Res.* **372**, 21–30.
55. Kubota Y. and Kawaguchi Y. (1993) Spatial distribution of chemically identified intrinsic neurons in relation to patch and matrix compartments of rat neostriatum. *J. comp. Neurol.* **332**, 499–513.
56. Langer L. F. and Graybiel A. M. (1989) Distinct nigrostriatal projection systems innervate striosomes and matrix in the primate striatum. *Brain Res.* **498**, 344–350.
57. Lavoie B. and Parent A. (1991) Dopaminergic neurons expressing calbindin in normal and parkinsonian monkeys. *NeuroReport* **2**, 601–611.
58. Levey A. I., Bolam J. P., Rye D. B., Hallanger A., Demuth R. M., Mesulam M.-M. and Wainer B. H. (1986) A light and electron microscopic procedure for sequential double antigen localization using diaminobenzidine and benzidine dihydrochloride. *J. Histochem. Cytochem.* **34**, 1449–1457.
59. Nastuk M. A. and Graybiel A. M. (1989) Ontogeny of M1 and M2 muscarinic binding sites in the striatum of the cat: relationships to one another and to striatal compartmentalization. *Neuroscience* **33**, 125–147.
60. Parent A., Fortin M., Côté P.-Y. and Cicchetti F. (1996) Calcium-binding proteins in primate basal ganglia. *Neurosci. Res.* **25**, 309–334.
61. Parent A. and Smith Y. (1987) Differential dopaminergic innervation of the two pallidal segments in the squirrel monkey (*Saimiri sciureus*). *Brain Res.* **426**, 397–400.
62. Paxinos A. and Watson C. (1986) *The Rat Brain in Stereotaxic Coordinates*. Academic Press, London.
63. Penny G. R., Wilson C. J. and Kitai S. T. (1988) Relationship of the axonal and dendritic geometry of spiny projection neurons to the compartmental organization of the neostriatum. *J. comp. Neurol.* **269**, 275–289.
64. Phend K. D., Weinberg R. J. and Rustioni A. (1992) Techniques to optimize post-embedding single and double staining for amino acid neurotransmitters. *J. Histochem. Cytochem.* **40**, 1011–1020.
65. Pickel V. M., Beckley S. C., Joh T. H. and Reis D. J. (1981) Ultrastructural immunocytochemical localization of tyrosine hydroxylase in the neostriatum. *Brain Res.* **225**, 373–385.
66. Ragsdale C. W. and Graybiel A. M. (1981) The fronto-striatal projection in the cat and monkey and its relationship to inhomogeneities established by acetylcholinesterase histochemistry. *Brain Res.* **208**, 259–266.
67. Rajakumar N., Elisevich K. and Flumerfelt B. A. (1993) Compartmental origin of the striato-entopeduncular projection in the rat. *J. comp. Neurol.* **331**, 286–296.
68. Rushlow W., Flumerfelt B. A. and Naus C. C. G. (1995) Colocalization of somatostatin, neuropeptide Y, and NADPH-diaphorase in the caudate-putamen of the rat. *J. comp. Neurol.* **351**, 499–508.
69. Shink E., Bevan M. D., Bolam J. P. and Smith Y. (1996) The subthalamic nucleus and the external pallidum: two tightly interconnected structures that control the output of the basal ganglia in the monkey. *Neuroscience* **73**, 335–357.
70. Smith A. D. and Bolam J. P. (1990) The neural network of the basal ganglia as revealed by the study of synaptic connections of identified neurones. *Trends Neurosci.* **13**, 259–266.
71. Smith Y. and Bolam J. P. (1989) Neurons of the substantia nigra reticulata receive a dense GABA-containing input from the globus pallidus in the rat. *Brain Res.* **493**, 160–167.
72. Smith Y. and Bolam J. P. (1991) Convergence of synaptic inputs from the striatum and the globus pallidus onto identified nigrocollicular cells in the rat: a double anterograde labelling study. *Neuroscience* **44**, 45–73.
73. Somogyi P. and Hodgson A. J. (1985) Antisera to γ -aminobutyric acid. III Demonstration of GABA in Golgi-impregnated neurons and in conventional electron microscopic sections of cat striate cortex. *J. Histochem. Cytochem.* **33**, 249–257.

74. Somogyi P., Hodgson A. J., Chubb I. W., Penke B. and Erdei A. (1985) Antisera to γ -aminobutyric acid. II Immunocytochemical application to the central nervous system. *J. Histochem. Cytochem.* **33**, 240–248.
75. Tepper J. M., Sawyer S. F. and Groves P. M. (1987) Electrophysiologically identified nigral dopaminergic neurons intracellularly labeled with HRP: light-microscopic analysis. *J. Neurosci.* **7**, 2794–2806.
76. van der Kooy D., Coscina D. V. and Hattori T. (1981) Is there a non-dopaminergic nigrostriatal pathway?. *Neuroscience* **6**, 345–357.
77. Veenman C. L., Reiner A. and Honig M. G. (1992) Biotinylated dextran amine as an anterograde tracer for single-labeling and double-labeling studies. *J. Neurosci. Meth.* **41**, 239–254.
78. von Krosigk M. and Smith A. D. (1991) Descending projection from the substantia nigra and retrorubral field to the medullary and pontomedullary reticular formation. *Eur. J. Neurosci.* **3**, 260–273.
79. Waldvogel H. J. and Faull R. L. M. (1993) Compartmentalization of parvalbumin immunoreactivity in the human striatum. *Brain Res.* **610**, 311–316.
80. Walker R. H., Arbuthnott G. W., Baughman R. W. and Graybiel A. M. (1993) Dendritic domains of medium spiny neurons in the primate striatum: relationships to striosomal borders. *J. comp. Neurol.* **337**, 614–628.
81. Walker R. H. and Graybiel A. M. (1993) Dendritic arbors of spiny neurons in the primate striatum are directionally polarized. *J. comp. Neurol.* **337**, 629–639.
82. Wise P. (1996) The role of the basal ganglia in procedural memory. *Semin. Neurosci.* **8**, 39–46.
83. Yamada T., McGeer P. L., Baimbridge K. G. and McGeer E. G. (1990) Relative sparing in Parkinson's disease of substantia nigra dopamine neurons containing calbindin-D28K. *Brain Res.* **526**, 303–307.
84. Zaborszky L., Cullinan W. E. and Braun A. (1991) Afferents to basal forebrain cholinergic projection neurons: an update. In *The Basal Forebrain* (ed Napier T. C.), pp. 43–100. Plenum Press, New York.
85. Zahm D. S. (1992) An electron microscopic morphometric comparison of tyrosine hydroxylase immunoreactive innervation in the neostriatum and the nucleus accumbens core and shell. *Brain Res.* **575**, 341–346.
86. Zhou M. and Grofova I. (1995) The use of peroxidase substrate Vector VIP in electron microscopic single and double antigen localization. *J. Neurosci. Meth.* **62**, 149–158.

(Accepted 23 April 1997)